Bonding in Ammonia Borane: An Analysis Based on the Natural Orbitals for Chemical Valence and the Extended Transition State Method (ETS-NOCV)

ARTICLE *in* THE JOURNAL OF PHYSICAL CHEMISTRY A · NOVEMBER 2011

Impact Factor: 2.69 · DOI: 10.1021/jp209712s · Source: PubMed

1 AUTHOR:

Mariusz Mitoraj
Jagiellonian University
54 PUBLICATIONS **1,162** CITATIONS

THE JOURNAL OF PHYSICAL CHEMISTRY A

ARTICLE

pubs.acs.org/JPCA

Bonding in Ammonia Borane: An Analysis Based on the Natural Orbitals for Chemical Valence and the Extended Transition State Method (ETS-NOCV)

Mariusz Paweł Mitoraj*

Department of Theoretical Chemistry, Faculty of Chemistry, Jagiellonian University, R. Ingardena 3, 30-060 Cracow, Poland

Supporting Information

ABSTRACT: In the present study the natural orbitals for chemical valence (NOCVs) combined with the energy decomposition scheme (ETS) were used to characterize bonding in various clusters of ammonia borane (borazane): dimer **D**, trimer **TR**, tetramer **TE**, and the crystal based models: nonamer **N** and tetrakaidecamer **TD**. ETS-NOCV results have shown that shortening of the B−N bond (by ∼0.1 Å) in ammonia borane crystal (as compared to isolated borazane molecule) is related to the enhancement of donation (by 6.5 kcal/mol) and electrostatic (by 11.3 kcal/mol) contributions. This, in turn, is caused *solely* by the electrostatic dipole−dipole interaction between ammonia borane units; dihydrogen bonding, BH···HN, formed between borazane units exhibits no direct impact on B−N bond contraction. On the other hand, formation of dihydrogen bonding appeared to be very important in the total stabilization of single borazane unit, namely, ETS-based data indicated that it leads to significant electronic stabilization $\Delta E_{orb} = -17.5$ kcal/mol, which is only slightly less important than the electrostatic term, $\Delta E_{elstat} = -19.4$ kcal/mol. Thus, both factors contribute to relatively high melting point of the borazane crystal. Deformation density contributions ($\Delta\rho_i$) obtained from NOCVs allowed to conclude that dihydrogen bonding is primarily based on outflow of electron density from B−H bonding orbitals to the empty σ^*(N−H) (charge transfer component). Equally important is the covalent contribution resulting from the shift of the electron density from hydrogen atoms of both NH and BH groups to the interatomic regions of NH···HB. Quantitatively, averaged electronic strength of dihydrogen bond per one BH···HN link varies from 1.95 kcal/mol (for the crystal structure model, **N**), 2.47 kcal/mol (for trimer **TR**), through 2.65 kcal/mol (for tetramer **TE**), up to 3.95 kcal/mol (for dimer **D**).

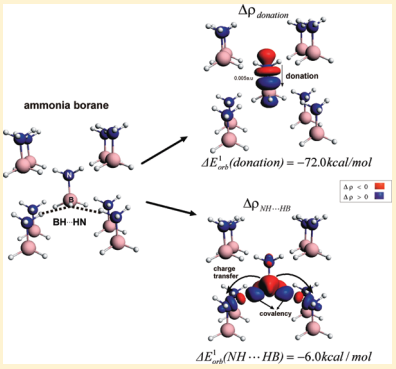

INTRODUCTION

Ammonia borane (AB), known also as borazane, is considered nowadays as one of the most promising hydrogen storage materials.[1,2,4−9] This is predominantly because of the large hydrogen storage capacity (19.6 wt % H_2). Another crucial factor is relatively high stability, even in higher temperature (the melting point is 104 °C), which is related to the character of bonding in AB.[1]

It has been observed a general trend that B−N bond length (1.58 Å) in the crystal structure is notably shorter as compared to isolated ammonia borane molecule (1.66 Å).[1,11,13,14] Such a decrease in the B−N bond length was initially attributed by Jonas et al. to electrostatic factor (short-range dipole−dipole interactions).[12] One year later Crabtree et al. suggested that somewhat untypical dihydrogen bonds, BH···HN, formed between borazane units are of the vital importance and the formation of a dihydrogen network could be the main factor contributing to the relatively high melting point of ammonia borane.[1,10] Popelier found on the basis of AIM study, by considering only dimeric structure of AB, that close contacts BH···HN are indeed stabilizing.[15,16] Morrison and Siddic predicted an average dihydrogen interaction energy of 12.7 kJ/mol (3.0 kcal/mol) by applying periodic DFT calculations.[17] In this work, however, no qualitative picture on the character of dihydrogen bonding was provided. The idea that dihydrogen bonding is the main factor contributing to high stability of AB was later contested by Merino et al., where authors explained the aggregation of ammonia borane molecules, leading to B−N bond shortening, on the basis of solely electrostatic factor.[11] In their work, however, authors considered the cluster models, where AB molecules are located in the aligned positions, that do not reflect real situation in the crystal (compare parts B and C of Figure 1).[1,13] On the other hand, *indirect* theoretical support for the electrostatic origin of B−N bond shortening was provided by Bühl et al. based on the analysis of bond length dependence in solvents characterized by different dielectric constants.[19]

Because of the above reasons, the main goal of this work is to characterize for the first time the bonding in various cluster models of ammonia borane and explaining B−N bond shortening in the crystal in terms of both *electrostatic* and *electronic*

Received: October 10, 2011
Revised: November 15, 2011
Published: November 15, 2011

dx.doi.org/10.1021/jp209712s | J. Phys. Chem. A 2011, 115, 14708–14716

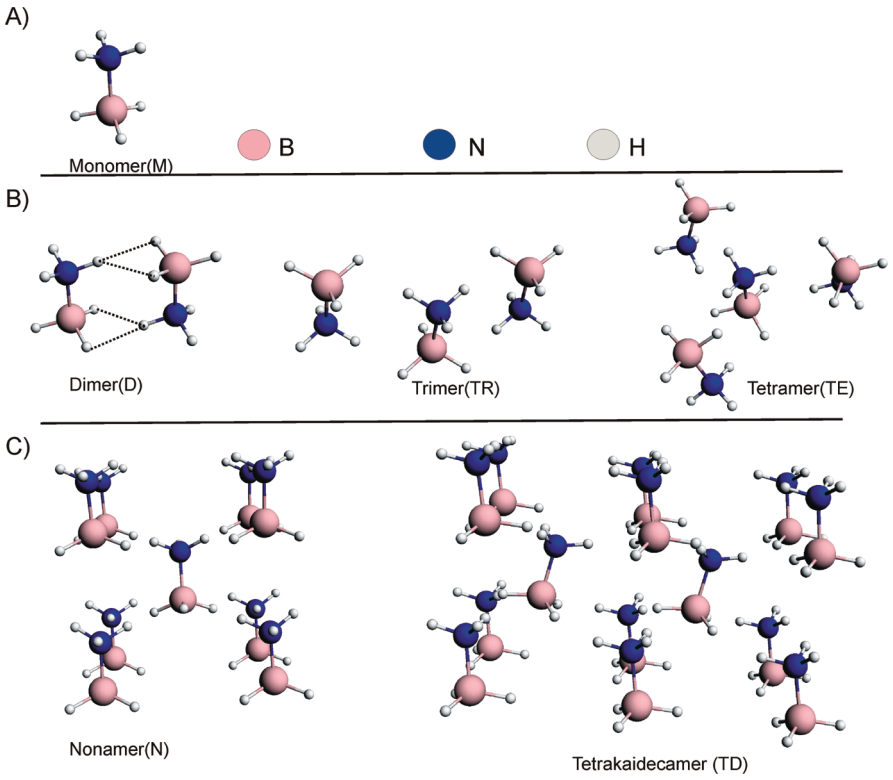

Figure 1. AB clusters studied in the present work together with their abbreviations. AB units situated in the aligned positions were considered in part B (analogous to these analyzed in ref 11), whereas real models obtained directly from the crystal structure are presented in part C. Example of dihydrogen bonds are marked in panel B.

contributions by applying the natural orbitals for chemical valence (NOCV) combined with the energy decomposition scheme (ETS).[20−24] It should be pointed out that quantitative role of these factors (electrostatic vs electronic) appears *directly* from ETS-NOCV analysis. In addition, the nature of dihydrogen bonds BH···HN formed between ammonia borane molecules will be characterized. It will be considered for the first time the cluster models *originating directly from the crystal structure* of *AB*, nonamer **N** and tetrakaidecamer **TD**. For comparison also dimeric (**D**), trimeric (**TR**), and tetrameric (**TE**) structures will be studied, see Figure 1.

As it has been already mentioned in the previous paragraph, we will use in the bonding analysis the ETS-NOCV method, which is a merger of energy decomposition method ETS[25,26] and NOCV scheme.[27−33] It was demonstrated that NOCVs allow for decomposition of the change in density upon bond formation ($\Delta\rho$) into different contributions ($\Delta\rho_k$) representing formation of specific bonding components, σ, π, δ, and polarizations.[20−24,27−33] Further, combination of NOCV methodology with the energy decomposition scheme ETS makes it possible to obtain the energy contributions ΔE_k^{orb} to bond energy from $\Delta\rho_k$.[20−24] Accordingly, ETS-NOCV offers a compact, qualitative (by providing deformation density contributions, $\Delta\rho_k$) and quantitative (by providing energetic estimations ΔE_k^{orb} for each $\Delta\rho_k$) picture of chemical bond formation within one common theoretical framework, even for molecules with no symmetry.[23]

COMPUTATIONAL DETAILS

All the DFT calculations presented here were based on the Amsterdam density functional (ADF) program.[34−36] The Becke−Perdew exchange-correlation functional[37,38] was applied. A standard double-ζ STO basis with one set of polarization functions was adopted for all atoms. Periodic calculations based on BAND program[39−41] were also performed in order to obtain B−N bond length in the crystal structure of AB. For comparison of stabilization energies also MP2 calculations (6-31G basis set) were performed using Gamess package.[42]

In the current study it has been considered the two types of analyses related to different fragmentation schemes.

At first place we have analyzed, with the help of ETS-NOCV method, the character of B−N bond in monomer; thus, the AB molecule was divided into ammonia (A) and borane (B) fragments. Further, to extract information on the changes in the character of B−N bond in the central AB molecule surrounded by other AB units (models of crystal structure), we have performed ETS-NOCV analysis in three fragments resolution, i.e., the interaction between ammonia (A), borane (B), and the rest of the cluster was considered, see Figure 2. Ammonia and borane fragments (red and green colors in Figure 2, respectively) were also marked separately by black continuous circles, whereas the remaining part of the cluster was identified by blue shadowed color. It will be shown that the NOCV-based approach allowed to separate useful qualitative and quantitative information on the electronic bonding *solely* between ammonia and borane subunits (black circle lines in Figure 2) *in the presence of remaining molecular environment* (blue shadowed color), whereas ETS analysis provided electrostatic contributions to B−N bond of the middle AB molecule (see nonamer in Figure 2). Thus, above procedure provides useful data that explains the origin of B−N bond shortening in the crystal comparing to monomer.

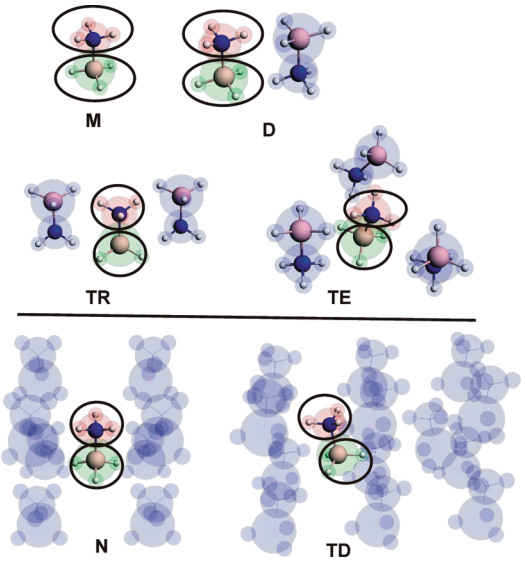

Figure 2. Fragmentation scheme used in ETS-NOCV analysis. In all cases (except monomer), the given model was divided into three fragments, i.e., ammonia, borane (black continuous circle lines), and the rest of the cluster (blue shadowed color).

Finally, the nature of dihydrogen bonding BH···HN was analyzed based on the two fragments resolution, i.e., the interaction between central AB molecule with the rest of the cluster was described. All considered molecular fragments were in the singlet ground state. Contours of deformation densities were plotted based on ADF-GUI interface.[43]

COMPUTATIONAL METHODS

Bonding analysis presented in this study is based on the ETS-NOCV approach, which is a combination of the extended transition state (ETS)[25,26] method with the NOCV scheme.[27−33]

Historically the NOCVs have been derived from the Nalewajski−Mrozek valence theory[44−46] as eigenvectors that diagonalize the deformation density matrix.[27−33] It was shown[27−33] that the NOCV pairs (ψ_{-k},ψ_k) decompose the differential density $\Delta\rho$ into NOCV contributions $(\Delta\rho_k)$

$$\Delta\rho(r) = \sum_{k=1}^{M/2} v_k[-\psi_{-k}^2(r) + \psi_k^2(r)] = \sum_{k=1}^{M/2} \Delta\rho_k(r) \quad (1)$$

where v_k and M stand for the NOCV eigenvalues and the number of basis functions, respectively. It has been shown that NOCV eigenvalues can provide *charge estimation*, $\Delta q_k = |v_k|$, of a given deformation density channel $\Delta\rho_k$. Visual inspection of deformation density plots $(\Delta\rho_k)$ helps to attribute symmetry and the direction of the charge flow. In addition, these pictures are enriched by providing the energetic estimations, ΔE_{orb}^k, for each $\Delta\rho_k$ within ETS-NOCV scheme. The exact formula which links ETS and NOCV method will be given in the next paragraph, after we briefly present the basic concept of ETS scheme. In this method the instantaneous interaction energy ΔE_{int} between fragments *exhibiting geometries as in the combined molecule* is divided into three components

$$\Delta E_{int} = \Delta E_{elstat} + \Delta E_{Pauli} + \Delta E_{orb} \quad (2)$$

The first term, ΔE_{elstat}, corresponds to the classical electrostatic interaction between the promoted fragments as they are brought to their positions in the final molecule. When considering three interacting fragments (A = ammonia, B = borane, C = rest of the cluster), the total electrostatic stabilization is an additive sum of each pair: $\Delta E_{elstat\text{-}total} = \Delta E_{elstat}(A-B) + \Delta E_{elstat}(A-C) + \Delta E_{elstat}(B-C)$. In the present study we will predominantly focus our attention on the stabilizing contribution originating from A−B interaction, $\Delta E_{elstat}(A-B)$, in the presence of third molecular fragment (C) (see Figure 2). The second term, ΔE_{Pauli}, accounts for the repulsive Pauli interaction between occupied orbitals on the fragments in the combined molecule. Finally, the last stabilizing term, ΔE_{orb}, represents the interactions between the occupied molecular orbitals of one fragment with the unoccupied molecular orbitals of the other fragments as well as mixing of occupied and virtual orbitals within the same fragment (inner-fragment polarization). This energy term may be linked to the electronic bonding effect coming from the formation of a chemical bond.

It should also be added that very often one might be interested in the *total interaction energy*, ΔE_{total}, between fragments exhibiting minima on the potential energy surface; in such a case it is needed to include the distortion term, ΔE_{dist}, that represents the amount of energy required to promote the separated fragments from their equilibrium geometry to the structure they will take up in the combined molecule; $-\Delta E_{total}$ value is known as bond dissociation energy (D_e)

$$\Delta E_{total} = \Delta E_{int} + \Delta E_{dist} = -D_e \quad (3)$$

In the combined ETS-NOCV scheme[20−24] the orbital interaction term (ΔE_{orb}) is expressed in terms of NOCV eigenvalues (v_k) as

$$\Delta E_{orb} = \sum_k \Delta E_{orb}^k = \sum_{k=1}^{M/2} v_k[-F_{-k,-k}^{TS} + F_{k,k}^{TS}] \quad (4)$$

where $F_{i,i}^{TS}$ are diagonal Kohn−Sham matrix elements defined over NOCV with respect to the transition state (TS) density (at the midpoint between density of the molecule and the sum of fragment densities). The above components ΔE_{orb}^k provide *energetic estimation* of $\Delta\rho_k$ that may be related to the importance of a particular electron flow channel for the bonding between considered molecular fragments.

RESULTS AND DISCUSSION

Let us first focus our attention on the electronic character of A−B bond of monomer that emerges from the ETS-NOCV scheme. It is evident from Figure 3 that dominant deformation density channel, $\Delta\rho_1$, originates from the electron donation from lone electron pair of ammonia to the lowest unoccupied orbital of BH_3. Such charge transfer corresponds to the highest energetic stabilization, $\Delta E_{orb}^1(A-B) = -65.5$ kcal/mol. The NOCVs indicated that the amount of charge transferred in this channel is $\Delta q_1 = 0.564$. The two quantitatively less crucial contributions to A−B bond, $\Delta\rho_2$ and $\Delta\rho_3$, with the corresponding energies, $\Delta E_{orb}^2(A-B) = -2.3$ kcal/mol and $\Delta E_{orb}^3(A-B) = -2.3$ kcal/mol, respectively, characterize π-back-donation channels, i.e., density outflow from occupied B−H orbitals (highest-occupied molecular orbital (HOMO) and HOMO-1) of borane to the empty $\sigma^*(N-H)$ of ammonia (lowest-unoccupied molecular orbital (LUMO)+1 and LUMO+2), see Figure 3. These transfers are associated with the flow of less amount of charge, $\Delta q_2 = \Delta q_3 = 0.136$.

Quantitative estimations of the strength of σ(A−B) and π(A−B) components are in good agreement with ETS based work by Bessac at al.[47] It should be added that charge depletion from B−H bonding orbitals is in line with the elongation of this bond, by 0.02 Å, compared to nonbonded borane molecule. Such elongation can originate from the "release" of Pauli repulsion between H-atoms due to reduction of the H−B−H angle (when going from planar BH_3 to tetrahedral conformation). Finally, the last contribution, $\Delta\rho_{rest}$, exhibiting both the back-donation channel ($BH_3 \rightarrow NH_3$) and polarization of BH_3 unit, gives rise to the stabilization ΔE^{rest}_{orb}(A−B) = −5.7 kcal/mol; it should be pointed out at this point that back-donation is realized by density outflow from deepest lying σ-orbital of BH_3 to higher-lying unoccupied σ-orbitals of ammonia. Nalewajski−Mrozek analysis have revealed that the B−N bond index is lower than one, 0.814, which is in line with general observations that donor−acceptor complexes exhibit usually weaker bonds as compared to typical single-bonded covalent molecules.[46]

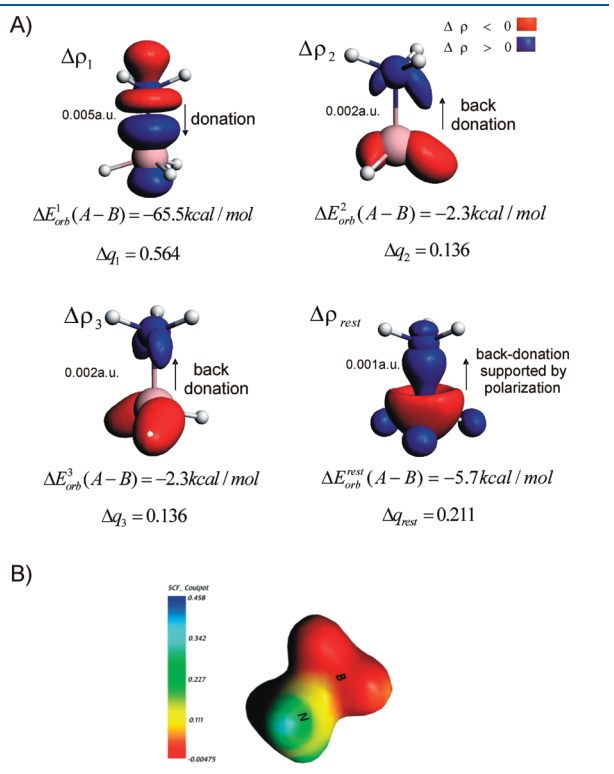

Figure 3. Contours of deformation density channels $\Delta\rho_1$, $\Delta\rho_2$, $\Delta\rho_3$, $\Delta\rho_4$ describing the bonding between ammonia and borane fragments in borazane, **M** (panel A). In addition the corresponding energy (ΔE^1_{orb}, ΔE^2_{orb}, ΔE^3_{orb}, ΔE^4_{orb}) and charge (Δq_1, Δq_2, Δq_3, Δq_4) estimations obtained from ETS-NOCV method are shown in panel A. In panel B the contour of electrostatic potential for NH_3BH_3 was presented.

All discussed already A−B bonding components originating from the charge flow channels give raise to the total orbital stabilization energy, $\Delta E_{orb\text{-}total}$ = −75.8 kcal/mol, see Table 1. Such significant donation leads to the gradient of charge distribution, what is reflected in the character of electrostatic potential, which becomes negative around BH_3 unit and positive around ammonia fragment, see part B of Figure 3. This also result in large dipole moment, by 5.4 D. Consequently, even higher stabilization from the electrostatic factor, $\Delta E_{elstat\text{-}total}$ = −76.9 kcal/mol, is observed for A−B bonding, see Table 1. Domination of the electrostatic component over electronic factor is in line with studies, by Mo et al.,[48] by Plumley et al.,[49] and by Jagielska et al.[50] An inclusion of the two other destabilizing bonding contributions (see eqs 2 and 3 in Computational Methods), i.e., Pauli repulsion (ΔE_{Pauli} = 108.0 kcal/mol) and distortion energy (ΔE_{dist} = 14.4 kcal/mol) terms, leads finally to the total bonding energy, ΔE_{total} = −30.3 kcal/mol. This value fits well to experimental enthalpy estimated by Haaland, −31.1 ± 1 kcal/mol[51,52] as well as to other theoretical estimations.[12,49] It has been shown by Dixon and Gutowski by applying very accurate CCSD(T) calculations that inclusion of zero-point energy correction leads to lower bond dissociation energy at 0 K, 25.9 and 27.7 kcal/mol at 298 K.[53] Jagielska et al. predicted 25.7 kcal/mol at 298 K,[50] whereas Bauschlicher and Ricca estimated lower value 24.6 kcal/mol at CCSD(T) level of theory.[54] Finally, one should summarize that σ-donation ($NH_3 \rightarrow BH_3$ charge transfer), electrostatic and the remaining (back-donation + polarization) components contribute to total stabilization of *A*−*B* bonding as much as 42.9, 50.4, and 6.7%, respectively.

An intriguing question arises at this point, namely, how the character of A−B bond will change upon surrounding of single AB molecule by eight other ammonia borane units? This reflects the real situation in the crystal structure of ammonia borane.[1,10] To answer this question, let us characterize the bonding in nonamer model (**N**) exhibiting the geometry as in the crystal, see part C of Figure 1. In Figure 4 the comparison of crucial

Table 1. ETS-NOCV-Based Results Comprising the Total Interaction between Three Fragments: Ammonia (A), Borane (B), and the Rest of the Cluster Together with the Contributions Stemming Solely from A−B Bonding

	ΔE^1_{orb}(A−B)	ΔE_{elstat}(A−B)	ΔE_{int}(A−B)[a]	$\Delta E_{orb\text{-}total}$	$\Delta E_{elstat\text{-}total}$	$\Delta E_{Pauli\text{-}total}$	$\Delta E_{int\text{-}total}$[b]	BN(BL/BO)[c]
M	−65.5	−76.9	−44.7	−75.8	−76.9	108.0	−44.7	1.660/0.814
D	−75.8	−82.1	−47.4	−96.9	−95.2	130.4	−61.7	1.634/0.828
TR	−84.6	−84.7	−49.7	−114.7	−109.9	147.2	−77.4	1.615/0.839
TE	−90.7	−86.5	−51.3	−127.0	−119.7	157.5	−89.2	1.603/0.846
N	−72.1	−84.3	−46.5	−98.0	−101.0	146.8	−52.2	1.626/0.831
TD	−69.2	−83.4	−47.0	−94.5	−98.3	146.0	−46.8	1.632/0.828
AB band[d]								1.594/0.835
crystal								1.584/0.860

[a] Interaction solely between ammonia and borane fragments (calculated from supermolecular approach). [b] ΔE_{int} = $\Delta E_{orb\text{-}total}$ + $\Delta E_{elstat\text{-}total}$ + $\Delta E_{Pauli\text{-}total}$. [c] BN bond lengths (BL) are in Ångstroms together with the Nalewajski−Mrozek bond order indices (BO). In all cases, with more than two AB molecules, B−N bond of central AB unit was characterized (see Figure 1). [d] Ammonia borane crystal structure obtained from periodic calculations using BAND program (BP86/TZ2P).

dx.doi.org/10.1021/jp209712s |*J. Phys. Chem. A* 2011, 115, 14708–14716

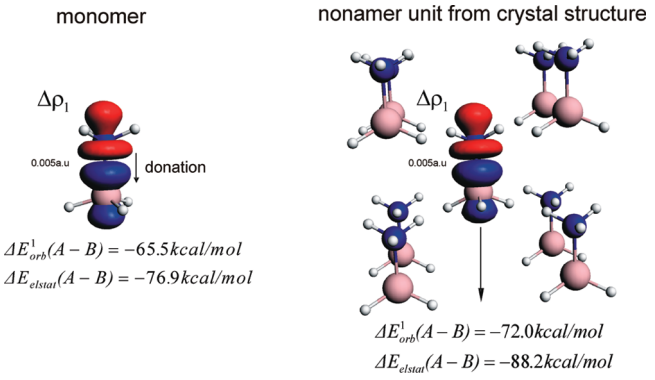

Figure 4. Contours of deformation density channels, $\Delta\rho_1$, describing donation A (ammonia)→borane (B) together with the corresponding energies, ΔE^1_{orb}(A−B), obtained from ETS-NOCV method. In addition the electrostatic component of A−B bond is shown.

stabilizing A−B bonding components for monomer (**M**) and nonamer (**N**) have been presented. First of all, it is gratifying to see that ETS-NOCV method, despite characterizing the interaction between three fragments (A, B, and rest of the cluster) in nonamer, allowed to separate and quantify the donation channel ($\Delta\rho_1$) describing solely central A−B bond, see Figure 4. It is clear from Figure 4 that donation has been enhanced (as compared to monomer), by 6.5 kcal/mol, upon the interaction with eight neighboring ammonia borane units. This is due to stronger overlap between orbitals involved in donation (HOMO of ammonia and LUMO of borane). In addition, it has been found that electrostatic stabilization between ammonia and borane subunits, ΔE_{elstat}(A−B), becomes even more negative, by 11.3 kcal/mol, for nonamer. Such higher stabilization originating from the electrostatic factor is related to stronger overlap of the two fragment densities. Both these factors (enhanced donation effect and stronger electrostatic stabilization) make the B−N bond of central AB shorter, by 0.08 Å, in the crystal structure. Such contraction correlate well with an increase in the Nalewajski−Mrozek B−N bond index from 0.814 for monomer up to 0.860 for the crystal structure, see Table 1. When considering fully optimized (at the level of BP86/TZ2P) structure of nonamer, similar trend, but less pronounced, is noted, i.e., bond order of B−N increases up to 0.831 (Table 1). A similar increase of bond order, up to 0.828, is noted for larger model, **TD**. Dillen and Verhoefen have shown based on MP2 calculations that B−N bond contraction in the crystal is in line with increase in B−N bond stretching frequency as well as with increase in the electron density at B−N bond critical point.[55] Merino at al.[11] and previously Jonas et al.[12] suggested that surrounded dipoles, AB fragments (see nonamer, **N**, in Figure 1c) induce the electric field in the central AB moiety that "pushes" the electron pair of N toward B and, thus, strengthens B−N bond. To verify the role of dipole environment numerical experiments based on nonamer model (**N**) have been performed in which eight surrounding ammonia borane units have been replaced by nonpolar ethane molecules; hence the environment does not exert, by the gradient of electric field, on the central AB moiety. It has been found, as a result of the geometry optimization, that the B−N bond length of the central AB unit increased from 1.58 Å (crystal structure) up to 1.64 Å (the same value as in isolated AB). In addition, dihydrogen bonds, H···H, between central AB and ethane molecules were broken (see Figure 1 of Supporting Information). These results evidently show that dipole environment is not only necessary for shortening of the B−N bond (because of an enhancement of the donation, ΔE^1_{orb}(A−B), and the electrostatic stabilization, ΔE_{elstat}(A−B)) but also for the existence of dihydrogen bonding $NH^{\delta+}\cdots^{\delta-}$HB. To further confirm the above observation, geometry optimizations of ammonia borane monomers surrounded from upper side by four point charges (each carrying +1) and from the lower side by four point charges (each carrying −1) have been performed. These point charges qualitatively represent the electrostatic environment (eight AB molecules, see section 2 of Supporting Information). It has been found that the B−N bond length of the monomer surrounded by point charges appeared to be analogous to that in the crystal (1.58 Å). Thus, necessary conditions leading to shortening of the B−N bond in the crystal are the presence of dipoles around "central" ammonia borane unit and at the same time no dihydrogen bonding (H···H) is needed. The presence of eight polar AB molecules as an environment also gives rise to the formation of dihydrogen bonds ($H^{\delta+}\cdots H^{\delta-}$), which certainly contributes to the relatively high melting point of ammonia borane. In the following paragraphs the character of dihydrogen bonds will be discussed based on ETS-NOCV scheme.

Table 2. ETS[a] Results (in kcal/mol) Characterizing the Stabilization Energy of Single AB Molecule in Various Clusters (D, TR, TE, N, See Figures 5−8 for Fragmentation Details Used in Bonding Analysis)

	ΔE_{orb}	ΔE_{elstat}	ΔE_{Pauli}	ΔE_{int} (BP86)	ΔE_{int} (MP2)
AB···AB(D)	−11.5	−20.3	17.3	−14.5	−16.1
AB···$(AB)_2$(TR)	−20.1	−37.7	30.9	−26.9	−31.2
AB···$(AB)_3$(TE)	−27.7	−49.6	39.3	−38.0	−44.8
AB···$(AB)_8$(N)	−17.5	−19.4	31.8	−5.1	−9.6

[a] $\Delta E_{int} = \Delta E_{orb} + \Delta E_{elstat} + \Delta E_{Pauli}$.

Considering the interaction between middle ammonia borane unit with the rest of the cluster, AB_8, in nonamer model (**N**), one might notice significant electrostatic stabilization (ΔE_{elstat} = −19.4 kcal/mol) due to dipole−dipole interaction; see the last row in Table 2. Domination of this factor is in line with the conclusion by Merino[11] (although their models do not reflect the real situation in the crystal structure). It has been found, however, based on ETS-NOCV methods that the *electronic stabilizing effect*, originating predominantly from the formation of dihydrogen bonds $NH^{\delta+}\cdots BH^{\delta-}$, *is only slightly less important* (ΔE_{orb} = −17.5 kcal/mol) *than the electrostatic term* (ΔE_{elstat} = −19.4 kcal/mol). Thus, both factors certainly contribute to relatively high melting point of the borazane crystal. Total stabilization energy of the central *AB* unit is ΔE_{int} = −5.1 kcal/mol (BP86 level of theory). More accurate MP2 calculations provided lower value of ΔE_{int} = −9.6 kcal/mol, which, in addition, suggests the existence of dispersion forces in the stabilization of single ammonia borane molecule, see nonamer in Table 2.

Let us now characterize the interaction of the middle ammonia borane unit with surrounding AB_8 clusters from the electronic point of view (eqs 1 and 4) based on the NOCV approach, see Figure 5. As it can be seen from Figure 5b three dominant deformation density channels capture the formation of dihydrogen connections (BH···HN) in nonamers $\Delta\rho_1$, $\Delta\rho_2$, $\Delta\rho_3$ with the corresponding energies ΔE^1_{orb} = −6.0 kcal/mol, ΔE^2_{orb} = −4.8 kcal/mol, and ΔE^3_{orb} = −1.1 kcal/mol, respectively. Qualitatively,

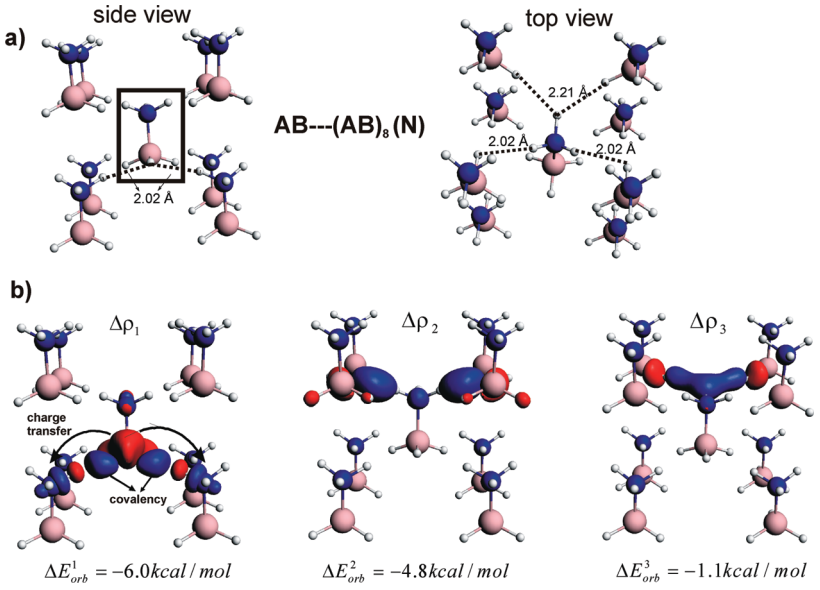

Figure 5. Fragmentation mode characterizing the interaction between middle ammonia borane unit (black square line) with rest of the cluster $(AB)_8$ is shown in panel **a**. In addition, selected close NH···HB contacts are shown from the side and top perspectives. In panel **b** the contours of deformation density channels, $\Delta\rho_1$, $\Delta\rho_2$, $\Delta\rho_3$, describing AB···$(AB)_8$ bonding are presented together with the corresponding energies.

the first charge transfer ($\Delta\rho_1$) channel involves outflow of electron density from B−H bonding orbitals of the middle AB unit to the empty σ^*(N−H) orbitals of two adjacent AB molecules (*charge transfer* label in Figure 5b). Similar charge transfer was noted for borazane dimer by Li and co-workers.[56] In addition, one can notice formation of the *covalent* components, i.e., the shift of electron density from hydrogen atoms of NH bonds (from two adjacent ABs) and BH unit (of central AB) to the interatomic regions of NH···HB is observed (see Figure 5b). Similar in qualitative nature are the charge transfers $\Delta\rho_2$ and $\Delta\rho_3$. It is noteworthy that the weakest (ΔE^3_{orb} = −1.1 kcal/mol) dihydrogen bonding BH···HN characterized by $\Delta\rho_3$ correlate well with the longest H···H distance (2.21 Å), see Figure 5a. An averaged *electronic* dihydrogen bond energy obtained from ETS-NOCV scheme per one BH···HN connection is ∼1.95 kcal/mol. Morrison and Siddic in their interesting study estimated *total* dihydrogen interaction energy to be ∼3.0 kcal/mol from the periodic DFT calculations. An important role of donor−acceptor interaction in dihydrogen bonded dimers has been recently deeply analyzed and understood by Hugas and co-workers.[57,58] Further, an involvement of the covalent component in hydrogen-bonded systems has been recently highlighted by Grabowski and co-workers.[59,60] It should be noticed, based on deformation density channels, that the covalent and charge transfer contributions to NH···HB bonding are qualitatively very similar to other typical hydrogen bonded systems (the only difference is that in the case of BH···NH bonding charge is donated not from the atomic fragment containing lone electron pair/s but from B−H bonding orbital).[57−61]

Finally, let us concisely characterize dihydrogen bonding in the smaller clusters **D**, **TR**, and **TE**, where ammonia borane units are located in the aligned position (thus they do not reflect the situation in borazane crystal); see Figures 6−8. It should be reminded that the presence of dihydrogen bonds can be important in terms of hydrogen release from ammonia borane. In their very elegant in-depth studies Dixon and co-workers analyzed the number of possible mechanistic pathways of release of hydrogen from ammonia borane dimer.[62,63] Qualitatively, in

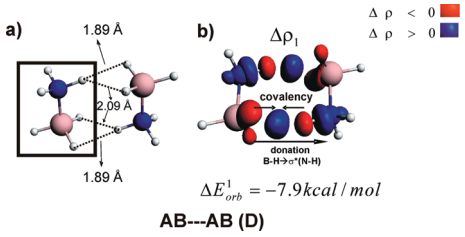

Figure 6. In panel **a** fragmentation of dimers into two ammonia borane molecules was presented together with NH···HB contacts. Contour of deformation density channel, $\Delta\rho_1$, together with the corresponding energy describing AB···AB bonding is shown in panel **b**.

each case (**D**, **TR**, **TE**), similarly to the nonamer model, one can observe formation of the covalent and charge-transfer contributions to BH···HN bond; see Figures 6b−8b. It is important to note that in the case of the trimer and tetramer nonequivalent dihydrogen bonds are present. More specifically, the two deformation density components, $\Delta\rho_1$ and $\Delta\rho_2$, corresponding to different stabilization energies ΔE^1_{orb} = −5.8 kcal/mol and ΔE^1_{orb} = −4.1 kcal/mol, respectively, constitute the bonding of middle AB with terminal $(AB)_2$ in trimer, see Figure 7. It nicely correlates with H···H distances; the longer the bond the weaker the electronic stabilization. Similar is true for the tetrameric cluster, although, differences in the strength of individual BH···HN connections are more pronounced; see Figure 8. Quantitatively, averaged electronic strength of dihydrogen bond per one BH···HN link varies from 2.47 kcal/mol (for **TR**) through 2.65 kcal/mol (for **TE**) up to 3.95 kcal/mol (for **D**). Finally, it should be summarized that averaged electronic strength of BH···HN dihydrogen bond is generally higher (2.47−3.95 kcal/mol) in the case of clusters containing aligned ammonia borane units (**D**, **TR**, **TE**) when compared to nonamer originating from the crystal structure (1.95 kcal/mol). In addition, the dominant role of the electrostatic factor over electronic term is far more evident

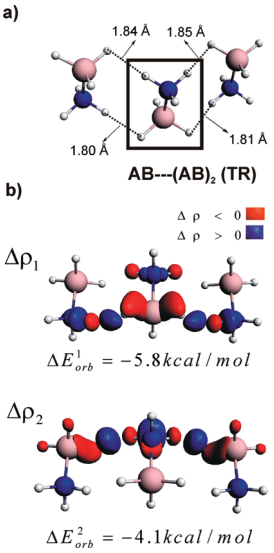

Figure 7. Fragmentation mode characterizing the interaction between middle ammonia borane unit (black square line) with the rest of the cluster $(AB)_2$ is shown in panel **a**. In addition, selected close NH···HB contacts are shown. In panel **b** the contours of deformation density channels, $\Delta\rho_1$ and $\Delta\rho_2$, describing AB···$(AB)_2$ bonding are shown together with the corresponding energies.

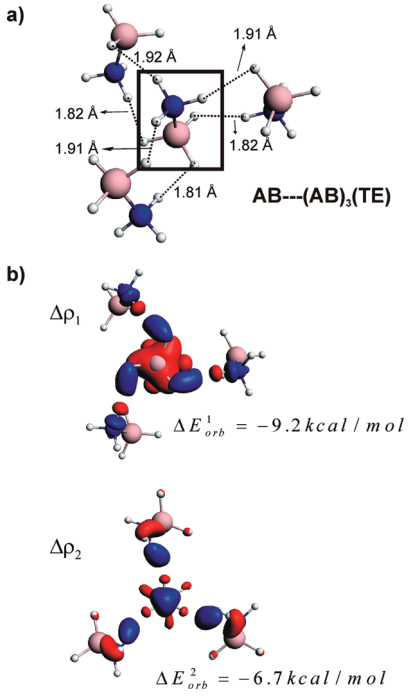

Figure 8. Fragmentation mode characterizing the interaction between middle ammonia borane unit (black square line) with the rest of the cluster $(AB)_3$ is shown in panel **a**. In addition, selected close NH···HB contacts are shown. In panel **b** the contours of deformation density channels, $\Delta\rho_1$ and $\Delta\rho_2$, describing AB···$(AB)_3$ bonding are shown together with the corresponding energies.

when considering aligned models (Table 2). Finally, the total stabilization energies (ΔE_{int}) of single borazane units are notably more negative for **D**, **TR**, and **TE** models as compared to nonamer (by 9.4−32.9 kcal/mol depending on the system). Our calculated value of the total stabilization energy for dimer is −14.5 kcal/mol (at BP86 level) and −16.1 kcal/mol (MP2 level), whereas −13.5 kcal/mol (with ZPE correction) was obtained by Nguyen and co-workers based on very accurate CCSD(T) data.[62]

CONCLUDING REMARKS

In the present study bonding in various cluster models of ammonia borane system (AB) (which is considered nowadays as very promising hydrogen storage material) has been charaterized by applying NOCVs combined with ETS. For the first time the models *originating directly from the crystal structure* of AB, nonamer **N** and tetrakaidecamer **TD**, were considered together with dimeric (**D**), trimeric (**TR**), and tetrameric (**TE**) structures. For a qualitative depiction of bonding components in ammonia borane clusters, the deformation density contributions, $\Delta\rho_k$, originating from NOCVs, have been used. To provide a quantitative picture of bonding, the ETS-NOCV scheme was applied to obtain energetic estimations, ΔE_k, associated with each charge rearrangement, $\Delta\rho_k$.

ETS-NOCV-based results indicated that shortening of the B−N bond (by ∼0.1 Å) in the ammonia borane crystal (as compared to isolated ammonia borane molecule) is directly related to the enhancement of donation ($NH_3 \rightarrow BH_3$) and electrostatic contributions. The latter effect appeared to be nearly double more important in the stabilization B−N bond. It has been proven based on nonamer model that such contraction of B−N connection should be associated solely with the electrostatic dipole−dipole interaction between "middle" AB molecule and surrounding other AB units, see Figure 1c. Dihydrogen bond formation, BH···HN between ammonia borane molecules appeared to exhibit no influence on the shortening of the B−N bond. However, formation of a dihydrogen network appeared to be very important as it leads to substantial stabilization of the single ammonia borane unit. It has been found based on ETS methods that such dihydrogen bonding stabilization (ΔE_{orb} = −17.5 kcal/mol) is only slightly less important than the stabilization originating from the electrostatic contribution (ΔE_{elstat} = −19.4 kcal/mol). Thus, both factors must contribute to the relatively high melting point of the borazane crystal. Further, MP2 results suggested that there exist dispersion forces between ammonia borane units. It has been proven, in addition, that necessary conditions for the existence of dihydrogen bonding is polar character of ammonia borane units; when replacing eight surrounding ammonia borane molecules in nonamer model by nonpolar ethane molecules, no dihydrogen connections were formed.

Finally, deformation density contributions ($\Delta\rho_i$) obtained from the ETS-NOCV scheme indicated that dihydrogen bonding between ammonia borane units is primarily based on outflow of electron density from B−H bonding orbitals to the empty σ^*(N−H) (charge transfer component). In addition, of similar importance is the covalent contribution formed by the shift of electron density from hydrogen atoms of both NH and BH bonds to the interatomic regions of NH···HB (see Figures 5b−8b). Quantitatively, averaged electronic strength of dihydrogen bond per one BH···HN link varies from 1.95 kcal/mol (for the crystal structure nonamer model, **N**), 2.47 kcal/mol (for trimer **TR**), through 2.65 kcal/mol (for tetramer **TE**), up to 3.95 kcal/mol (for dimer **D**).

■ ASSOCIATED CONTENT

Supporting Information. Cartesian coordinates for the analyzed structures as well as the results for ethane-based nonamer and monomer with point charges. This material is available free of charge via the Internet at http://pubs.acs.org.

■ AUTHOR INFORMATION

Corresponding Author
*E-mail: mitoraj@chemia.uj.edu.pl.

■ ACKNOWLEDGMENT

Mariusz P. Mitoraj greatly acknowledges the financial support from Polish Ministry of Science and Higher Education (for "Outstanding Young Researchers" Scholarships, 2010, 2011-2014, and for young researchers T-subsidy).

■ REFERENCES

(1) Staubitz, A.; Robertson, A. P. M.; Manners, I. *Chem. Rev.* **2010**, *110*, 4079.
(2) Smythe, N. C.; Gordon, J. C. *Eur. J. Inorg. Chem.* **2010**, 509.
(3) Stephens, F. H.; Pons, V.; Baker, R. T. *Dalton Trans.* **2007**, 2613.
(4) Hamilton, C. W.; Baker, R. T.; Staubitz, A.; Manners, I. *Chem. Soc. Rev.* **2009**, *38*, 279.
(5) Denney, M. C.; Pons, V.; Hebden, T. J.; Heinekey, D. M.; Goldberg, K. I. *J. Am. Chem. Soc.* **2006**, *128*, 12048.
(6) Käss, M.; Friedrich, A.; Drees, M.; Schneider, S. *Angew. Chem., Int. Ed.* **2009**, *48*, 905.
(7) Blaquiere, N.; Diallo-Garcia, S.; Gorelsky, S. I.; Black, D. A.; Fagnou, K. *J. Am. Chem. Soc.* **2008**, *130*, 14034.
(8) Keaton, R. J.; Blacquiere, J. M.; Baker, R. T. *J. Am. Chem. Soc.* **2007**, *129*, 1844.
(9) Kim, S.-K.; Han, W.-S.; Kim, T.-J.; Kim, T.-Y.; Nam, S. W.; Mitoraj, M.; Piękoś, Ł.; Michalak, A.; Hwang, S.-J.; Kang, S. O. *J. Am. Chem. Soc.* **2010**, *132*, 9954.
(10) Richardson, T. B.; de Gala, S.; Crabtree, R. H. *J. Am. Chem. Soc.* **1995**, *117*, 12875.
(11) Merino, G.; Bakhmutov, V. I.; Vela, A. *J. Phys. Chem. A.* **2002**, *106*, 8491.
(12) Jonas, V.; Frenking, G.; Reetz, M. T. *J. Am. Chem. Soc.* **1994**, *116*, 8741.
(13) Klooster, W. T.; Koetzle, T. F.; Siegbahn, P. E. M.; Richardson, T. B.; Crabtree, R. H. *J. Am. Chem. Soc.* **1999**, *121*, 6337.
(14) Thorne, L. R.; Suenram, R. D.; Lovas, F. J. *J. Chem. Phys.* **1983**, *78*, 167.
(15) Bader, R. F. W. *Atoms in Molecules: A Quantum Theory*; Oxford University Press: Oxford, U.K., 1990.
(16) Popelier, P. L. A. *J. Phys. Chem. A.* **1998**, *102*, 1873.
(17) Morrison, A. M.; Siddick, C. A. *Angew. Chem., Int. Ed.* **2004**, *43*, 4780.
(18) Hoon, C.; Reynhard, E. C. *J. Phys. C* **1983**, *16*, 6129.
(19) Bühl, M.; Steinke, T.; Schleyer, P.v. R.; Boese, R. *Angew. Chem., Int. Ed.* **1991**, *30*, 1160.
(20) Mitoraj, M.; Michalak, A; Ziegler, T. *J. Chem. Theory Comput.* **2009**, *5* (4), 962.
(21) Mitoraj, M.; Michalak, A; Ziegler, T. *Organometallics* **2009**, *28* (13), 3727.
(22) Mitoraj, M.; Michalak, A *Inorg. Chem.* **2011**, *50*, 2168.
(23) Brocławik, E.; Mitoraj, M.; Rejmak, P.; Michalak, A. *Handbook of Inorganic Chemistry Research*; Columbus, F.; Nova Publisher: New York, 2010; pp 361−383.
(24) Babashkina, M. B.; Safin, D. A.; Bolte, M.; Srebro, M.; Mitoraj, M.; Uthe, A.; Klein, A.; Ködkerling, M. *Dalton Trans.* **2011**, *40*, 1.
(25) Ziegler, T.; Rauk, A. *Inorg. Chem.* **1979**, *18*, 1755.
(26) Ziegler, T.; Rauk, A. *Inorg. Chem.* **1979**, *18*, 1558.
(27) Mitoraj, M.; Michalak, A. *J. Mol. Model.* **2007**, *13*, 347.
(28) Michalak, A.; Mitoraj, M.; Ziegler, T. *J. Phys. Chem. A.* **2008**, *112* (9), 1933.
(29) Mitoraj, M.; Michalak, A. *Organometallics* **2007**, *26* (26), 6576.
(30) Mitoraj, M.; Michalak, A. *J. Mol. Model.* **2008**, *14*, 681.
(31) Mitoraj, M.; Zhu, H.; Michalak, A.; Ziegler, T. *Int. J. Quantum Chem.* **2008**, DOI: 10.1002/qua.21910.
(32) Srebro, M; Mitoraj, M. *Organometallics* **2009**, *28* (13), 3650.
(33) Srebro, M; Michalak, A *Inorg. Chem.* **2009**, *48* (12), 5361.
(34) TeVelde, G; Bickelhaupt, F. M.; Baerends, E. J.; Fonseca Guerra, C.; Van Gisbergen, S. J. A.; Snijders, J. G.; Ziegler, T. *J. Comput. Chem.* **2001**, *22*, 931.Baerends, E. J.; Autschbach, J.; Bashford, D.; Bérces, A.; Bickelhaupt, F. M.; Bo, C.; Boerrigter, P. M.; Cavallo, L.;Chong, D. P.; Deng, L.; Dickson, R. M.; Ellis, D. E.; van Faassen, M.; Fan, L.; Fischer, T. H.; Fonseca Guerra, C.; Ghysels, A.; Giammona, A.; van Gisbergen, S. J. A.; Götz, A. W.; Groeneveld, J. A.; Gritsenko, O. V.; Grüning, M.; Harris, F. E.; van den Hoek, P.; Jacob, C. R.; Jacobsen, H.; Jensen, L.; van Kessel, G.; Kootstra, F.; Krykunov, M. V.; van Lenthe, E.; McCormack, D. A.; Michalak, A.; Mitoraj, M.; Neugebauer, J.; Nicu, V. P.; Noodleman, L.; Osinga, V. P.; Patchkovskii, S.; Philipsen, P. H. T.; Post, D.; Pye, C. C.; Ravenek, W.; Rodríguez, J. I.; Ros, P.; Schipper, P. R. T.; Schreckenbach, G.; Seth, M.; Snijders, J. G.; Solà, M.; Swart, M.; Swerhone, D.; te Velde, G.; Vernooijs, P.; Versluis, L.; Visscher, L.; Visser, O.; Wang, F.; Wesolowski, T. A.; van Wezenbeek, E. M.; Wiesenekker, G.; Wolff, S. K.; Woo, T. K.; Yakovlev, A. L.; Ziegler, T. *ADF2009.01*; Theoretical Chemistry; Vrije Universiteit: Amsterdam.
(35) Baerends, E. J.; Ellis, D. E.; Ros, P. *Chem. Phys.* **1973**, *2*, 41.
(36) te Velde, G.; Baerends, E. J. *J. Comput. Phys.* **1992**, *99*, 84.
(37) Becke, A. *Phys. Rev. A* **1988**, *38*, 3098.
(38) Perdew, J. P. *Phys. Rev. B* **1986**, *34*, 7406.
(39) Philipsen, P. H. T.; G. te Velde, Baerends, E. J.; Berger, J. A.; P. L. de Boeij, Groeneveld, J. A.; Kadantsev, E. S.; Klooster, R.; Kootstra, F.; Romaniello, P.; Skachkov, D. G.; Snijders, J. G.; Wiesenekker, G.; Ziegler, T. *BAND2010*; SCM, Theoretical Chemistry, Vrije Universiteit, Amsterdam, The Netherlands, http://www.scm.com.
(40) te Velde, G.; Baerends, E. J. *Phys. Rev. B* **1991**, *44*, 7888.
(41) Wiesenekker, G.; Baerends, E. J. *J. Phys.: Condens. Matter* **1991**, *3*, 6721.
(42) Schmidt, M. W.; Baldridge, K. K.; Boatz, J. A.; Elbert, S. T.; Gordon, M. H.; Jensen, J. H.; Koseki, S.; Matsunaga, N.; Nguyen, K. A.; Su, S.; Windus, T. L.; Dupuis, M.; Montgomery, J. A. *J. Comput. Chem.* **1993**, *14*, 1347.
(43) Visser, O.; Leyronnas, P.; van Zeist, W.-J.; Lupki, M. *ADF-GUI 2009.01*, SCM, Amsterdam, The Netherlands, http://www.scm.com.
(44) Nalewajski, R. F.; Mrozek, J.; Michalak, A. *Int. J. Quantum Chem.* **1997**, *61*, 589.
(45) Nalewajski, R. F.; Mrozek, J.; Michalak, A. *Pol. J. Chem.* **1998**, *72*, 1779.
(46) Michalak, A.; De Kock, R.; Ziegler, T. *J. Phys. Chem. A* **2008**, *112*, 7256.
(47) Bessac, F.; Frenking, G. *Inorg. Chem.* **2006**, *45*, 6956.
(48) Mo, Y.; Song, L.; Wu, W.; Zhang, Q. *J. Am. Chem. Soc.* **2004**, *126*, 3974.
(49) Plumley, J. A.; Evanseck, J. D. *J. Phys. Chem. A.* **2007**, *111*, 13472and references therein..
(50) Jagielska, A.; Moszynski, R.; Piela, L. *J. Chem. Phys.* **1999**, *110*, 947.
(51) Halaand, A. *Angew. Chem., Int. Ed.* **1989**, *101*, 1017.
(52) Halaand, A. *Angew. Chem., Int. Ed.* **1989**, *28*, 992.
(53) Dixon, D. A.; Gutowski, M. *J. Phys. Chem. A* **2005**, *109*, 5129.
(54) Bauschlicher, C. W.; Ricca, A., Jr. *Chem. Phys. Lett.* **1995**, *14*, 237.
(55) Dillen, J.; Verhoeven, P. *J. Phys. Chem. A* **2003**, *107*, 2570.
(56) Li, J.; Zhao, F.; Jing, F. *J. Chem. Phys.* **2002**, *116*, 25.
(57) Hugas, D.; Simon, S.; Duran, M.; Guerra, C. F.; Bickelhaupt, F. M. *Chem.—Eur. J.* **2009**, *15*, 5814.

(58) Hugas, D.; Simon, S.; Duran, M. *J. Phys. Chem. A* **2007**, *111*, 4506.
(59) Grabowski, S. J. *Chem. Rev.* **2011**, *111*, 2597.
(60) Grabowski, S.; Sokalski, A.; Leszczynski, J. *J. Phys. Chem. A* **2005**, *109*, 4331.
(61) Kurczab, R.; Mitoraj, M. P.; Michalak, A.; Ziegler, T. *J. Phys. Chem. A* **2010**, *114* (33), 8581.
(62) Nguyen, V. S.; Matus, M. H.; Grant, D. J.; Nguyen, M. T.; Dixon, D. A. *J. Phys. Chem. A* **2007**, *111*, 8844.
(63) Matus, M. H.; Grant, D. J.; Nguyen, M. T.; Dixon, D. A. *J. Phys. Chem. C* **2009**, *113*, 16553.